The iron-responsive element (IRE)/iron-regulatory protein 1 (IRP1)–cytosolic aconitase iron-regulatory switch does not operate in plants

Nicolas ARNAUD[1], Karl RAVET[1], Andrea BORLOTTI[2], Brigitte TOURAINE, Jossia BOUCHEREZ, Cécile FIZAMES, Jean-François BRIAT, Françoise CELLIER and Frédéric GAYMARD[3]

Laboratoire de Biochimie et Physiologie Moléculaire des Plantes, UMR 5004 Agro-M/CNRS/INRA/UMII, Bat 7, 2 place Viala, 34060 Montpellier cedex 1, France

Animal cytosolic ACO (aconitase) and bacteria ACO are able to switch to RNA-binding proteins [IRPs (iron-regulatory proteins)], thereby playing a key role in the regulation of iron homoeostasis. In the model plant *Arabidopsis thaliana*, we have identified three IRP1 homologues, named ACO1–3. To determine whether or not they may encode functional IRP proteins and regulate iron homoeostasis in plants, we have isolated loss-of-function mutants in the three genes. The *aco1-1* and *aco3-1* mutants show a clear decrease in cytosolic ACO activity. However, none of the mutants is affected in respect of the accumulation of the ferritin transcript or protein in response to iron excess. *cis*-acting elements potentially able to bind to the IRP have been searched for *in silico* in the *Arabidopsis* genome. They appear to be very rare sequences, found in the 5′-UTR (5′-untranslated region) or 3′-UTR of a few genes unrelated to iron metabolism. They are therefore unlikely to play a functional role in the regulation of iron homoeostasis. Taken together, our results demonstrate that, in plants, the cytosolic ACO is not converted into an IRP and does not regulate iron homoeostasis. In contrast with animals, the RNA binding activity of plant ACO, if any, would be more likely to be attributable to a structural element, rather than to a canonical sequence.

Key words: *Arabidopsis thaliana*, cytosolic aconitase, ferritin, iron homoeostasis, iron-regulatory protein 1 (IRP1), reactive oxygen species (ROS).

INTRODUCTION

As the major cofactor of proteins involved in essential processes like photosynthesis, respiration, DNA replication or nitrogen fixation, iron is an essential element for life. Nonetheless, in the free ionic form, iron is toxic, as it can catalyse the formation of ROS (reactive oxygen species) through the Fenton reaction. These ROS damage the cell membranes, DNA and proteins [1,2]. Thus iron homoeostasis has to be tightly regulated to avoid starvation that impairs the metabolism and to avoid excess that may lead to cell death. Iron homoeostasis is strongly dependent on ferritins, which are iron-storage proteins found in bacteria, animals and plants. Plant and animal ferritin structures are very similar and are formed by 24 subunits arranged to form a hollow sphere able to sequester iron in a non-toxic and bioavailable form [3].

A major regulatory pathway of iron homoeostasis in multicellular eukaryotic organisms has been documented from studies with animal systems [3,4]. In these systems, the balance between iron uptake and iron storage is mainly achieved by the post-transcriptional regulation of ferritin and transferrin receptor synthesis by the IRE (iron-responsive element)/IRP1 (iron-regulatory protein 1)–cytosolic ACO (aconitase) iron switch. In the 5′-UTR (5′-untranslated region) of ferritin mRNA and in the 3′-UTR of transferrin receptor transcripts are located specific sequences, termed IREs [5]. The IREs function as binding sites for two related *trans*-acting factors, namely IRP1 and IRP2. When bound to the IRE of the ferritin mRNA, the IRP inhibits translation of the transcript [4]. Conversely, the binding of IRP to the IREs found in the 3′-untranslated sequence of the transferrin receptor mRNA stabilizes the transcript, leading to the synthesis of the protein.

IRP1 is a bifunctional protein that, when iron is abundant, possesses a 4Fe-4S cluster and acts as a cytosolic ACO. When the iron level is low, the 4Fe-4S cluster disassembles and the apoprotein acquires IRP activity, thus repressing ferritin translation. High levels of iron lead to the 4Fe-4S cluster reconstitution and therefore to the protein ACO activity. Exposure to NO (nitric oxide) and ROS was shown to convert the ACO into an IRP by releasing the cluster, consequently leading to the IRE binding, and finally modulating the expression of ferritins [6,7]. IRP2 is an IRP1 homologue that does not contain an Fe-S cluster and thus has no ACO activity. Its activity is primarily regulated by iron-dependent degradation [8].

Several reports suggested that the IRE/IRP1–cytosolic ACO switch could also operate in plants [9–11], making it a universal regulatory pathway in eukaryotic pluricellular organisms. Indeed, several lines of evidence suggest a putative relation between ferritins and ACO activity. NO and oxidative stress have been shown to modulate the expression of ferritins in plants [11–13] and to inactivate the ACO [10,14], thus potentially converting it into an IRP. However, indirect lines of evidence are not in favour of an IRE/IRP1–cytosolic ACO regulatory switch in plants. Indeed, the synthesis of plant ferritins and iron transporters has been shown to be regulated at the transcriptional level in response to the iron status, and not at the mRNA stability or translational levels as described above for animal cells [12,15]. IRE sequences are not found in the plant ferritin genes. No IRP activity is detectable in plant cell extracts by RNA shift experiments using animal IRE as a probe [16] or in a translational assay using animal ferritin mRNA and wheatgerm extract [17]. However, it must be pointed out that the bacterial ACO does have an RNA binding

Abbreviations used: ACO, aconitase; DTNB, 5,5′-dithiobis-(2-nitrobenzoic acid); IRE, iron-responsive element; IRP, iron-regulatory protein; NO, nitric oxide; ROS, reactive oxygen species; T-DNA, transfer DNA; TNB-SH, 2-nitro-5-thiobenzoic acid reduced form; UTR, untranslated region.

[1] These authors contributed equally to this work.

[2] Present address: Dipartimento di Produzione Vegetale, Università degli Studi di Milano, Via Celoria, 2, 20133 Milano, Italy.

[3] To whom correspondence should be addressed (email gaymard@supagro.inra.fr).

activity, but does not recognize a canonical IRE sequence [18,19]. The potential RNA binding activity of plant ACO was recently underscored by the observation that an *Arabidopsis* ACO protein was able to bind to the 5′-UTR of the superoxide dismutase *CSD2* gene [20].

In order to directly address the involvement of a putative IRP1–cytosolic ACO regulatory switch in the regulation of ferritin expression in plants, we searched for IRP homologues in the *Arabidopsis* genome, identified three genes encoding putative ACO and isolated the corresponding loss-of-function mutants. In the three mutants, the expression of genes involved in iron homoeostasis was not altered, demonstrating that cytosolic ACO, in contrast with the situation in animals and bacteria, is not involved in the regulation of iron metabolism in plants.

EXPERIMENTAL

Isolation of *aco* knockout mutants

Mutants in the three ACO genes *ACO1* (At4g35830), *ACO2* (At4g26970) and *ACO3* (At2g05710) were identified in the collections from the Salk Institute [21] for *ACO2* (line Salk-054196) and *ACO3* (line Salk-013368) and from the GABI-Kat [22] for *ACO1* (line 138A08). Plants were back-crossed and homozygous mutant plants were identified by PCR on genomic DNA. The two T-DNA (transfer DNA)–gene junctions were amplified and sequenced to determine the location of the T-DNA insertion.

Plant culture

Arabidopsis plants were grown on soil (Humin substrate N2 Neuhaus; Klasmann-Deilmann, Geeste, Germany) in a greenhouse at 23 °C with a light intensity maintained above 300 $\mu E \cdot s^{-1} \cdot m^{-2}$ and a day/night regime of 16 h/8 h. For determining the expression pattern of *ACO* genes, wild-type (Col ecotype) plants were grown under hydroponic conditions for 5 weeks as described in [23]. The other studies were performed on 10-day-old plantlets grown in liquid medium under sterile conditions [13]. For the iron-starvation treatment, plants were transferred to the same medium, except that Fe(III)-EDTA was omitted. For iron excess treatment, a mix of $FeSO_4$/trisodium citrate was added (final concentration in the medium: 300 μM $FeSO_4$/600 μM trisodium citrate).

RNA preparation and analysis

Total RNA was extracted, and Northern blot experiments were performed as described by Lobréaux et al. [24]. The *EF1α*-, *AtFer1*- and *IRT1*-specific probes were obtained as described in [13,25]. The *AtFer3*-specific probe consists in a chimaeric fragment containing the 5′- and 3′-UTR of the *AtFer3* cDNA. The 5′-UTR was amplified with thermostable Pfu DNA polymerase (Promega, Madison, WI, U.S.A.) by using the primers 5′-GGTACCTATATTCCCTCCTCCGCCACCACCAATC-3′ and 5′-GAATTCAAACCGGAGACGAAATGGAGG-3′ introducing a KpnI and an EcoRI site at the 5′- and 3′-ends of the amplified fragment respectively. The 3′-UTR was amplified by using the primers 5′-TGGGAATTCTGCTTAATCTGAG-3′ and 5′-GGGTACTAGTAAATATCAGTG-3′ introducing an EcoRI and an SpeI site at the 5′- and 3′-ends of the amplified fragment respectively. The fragment was cloned at the corresponding sites in pBluescript and sequenced. The specific probe (462 bp) was obtained by digesting the resulting construct with KpnI and SpeI. The *ACO*-specific probes were amplified by PCR on genomic DNA as described above for *AtFer3*, cloned in pBluescript at the EcoRV site, and sequenced. The *ACO1* probe, located in the 3′-UTR, was amplified with the primers 5′-GAGTTGGCTTATTTCGATCAGG-3′ and 5′-GACTCGACAGTGATAATGTTTCC-3′. The two other *ACO* probes, located in the 5′-UTR, were amplified with 5′-CTTGACGAAATCTCTTCTCCGTCTC-3′ and 5′-GAGCAAACTCGAAAGGAGCGGAGAGCC-3′ for *ACO2*, and 5′-CGCAGCCCTAGGCATTTTCG-3′ and 5′-GGGGAAATGGTACCAAAAGATCTACG-3′ for *ACO3*. The *25S* RNA and specific probes were labelled, and hybridization was performed as described in [13].

Preparation of cytosolic and mitochondrial matrix extracts

All procedures were carried out at 4 °C. Plantlets (50 g) were cut with a razor blade and ground in a mortar containing extraction buffer (330 mM sorbitol, 30 mM Mops/Bis-Tris propane, 2 mM PMSF, 2 mM 2-mercaptoethanol, 2 mM trisodium citrate, 2 mM ascorbic acid, 1 mM EDTA, 10 $\mu g \cdot ml^{-1}$ leupeptin and 1 % polyvinylpyrrolidone, pH 7.5) in the ratio 1:3 (w/v). The homogenate was filtered through two layers of Miracloth (Calbiochem, Merck Biosciences; Darmstadt, Germany), and centrifuged at 280 ***g*** for 10 min to remove the cell debris and the chloroplasts. The supernatant was centrifuged at 10 800 ***g*** for 30 min. The resulting pellet contained mitochondria, while the supernatant corresponded to the cytosol and the membrane fractions. This supernatant was centrifuged at 100 000 ***g*** for 45 min to pellet the membranes. Glycerol [final concentration 10 % (v/v)] was added to the resulting supernatant (cytosolic fraction), and samples were stored in liquid nitrogen until use. The pellet containing mitochondria was resuspended in 2 ml of lysis buffer (10 mM Tris/HCl, 2 mM 2-mercaptoethanol, 2 mM trisodium citrate, 1 mM PMSF, 1 mM EDTA and 10 $\mu g \cdot ml^{-1}$ leupeptin, pH 7.2). Mitochondria were broken by vortex-mixing and freezing three times the samples in liquid nitrogen. After a centrifugation at 100 000 ***g*** for 45 min, the supernatant containing matrix proteins was recovered. Glycerol (final concentration 10 %) was added, and samples were stored in liquid nitrogen. Protein concentration was determined as described by Schaffner and Weissmann [26] by using BSA as the standard.

Enzymatic activities

ACO activity was assayed at 20 °C in 100 mM Tris/HCl and 50 mM DL-isocitric acid (trisodium salt) (pH 7.4) by measuring the production of *cis*-aconitate. The molar absorption coefficient used for *cis*-aconitate was 3.6 $mM^{-1} \cdot cm^{-1}$ at 240 nm. The reaction was started by adding from 75 to 150 μg of protein in 1 ml final volume. Before measuring the citrate synthase activity, mitochondrial and cytosolic extracts were purified in a BioSpin 6 column (Bio-Rad, Hercules, CA, U.S.A.), following the manufacturer's instructions, to remove the 2-mercaptoethanol that negatively influences the activity. Citrate synthase activity was determined in 100 mM Tris/HCl, 0.1 mM DTNB [5,5′-dithiobis-(2-nitrobenzoic acid)] and 0.2 mM acetyl-CoA (pH 8.0) from 50 μg of protein extract in 1 ml final volume. After 5 min of incubation at 30 °C, the reaction was initiated by adding oxaloacetic acid (1 mM final concentration) at room temperature (20 °C). The reduction of DTNB was measured by detection of TNB-SH (2-nitro-5-thiobenzoic acid reduced form). The molar absorption coefficient used for TNB-SH was 13.8 $mM^{-1} \cdot cm^{-1}$ at 412 nm.

Immunodetection of ferritins

Total protein extracts were prepared from 1 g of each sample as described in [27]. Proteins were subjected to electrophoresis on a 13 % polyacrylamide/0.1 % SDS gel by the method of Laemmli [28]. After electroblotting on to Hybond-P membrane (Amersham

Biosciences), immunodetection of ferritin was performed by using a rabbit polyclonal antiserum raised against purified AtFer1 protein [29] and the Aurora Western blotting kit (MP Biomedicals, Irvine, CA, U.S.A.) following the manufacturer's recommendations.

Bioinformatics

IRE motif searches were performed on *Arabidopsis thaliana* 5′- and 3′-UTR sequences [available at TAIR (The *Arabidopsis* Information Resource) website http://www.arabidopsis.org/] by using a Perl script specially written for this purpose, and by using the sequence CXXXXXCAGUGNYYYYY as consensus of the IRE loop. The constraints imposed in the script were as follows: N designates any of the four bases. The five bases noted X and Y are involved in the stem formation, and must be complementary (A/U, C/G) or form a stable weak interaction (U/G). For the putative bacterial *acn*-binding site, the two paired motifs, ACACAAUGC and CAUUUU, as defined by Tang and Guest [18], were searched. To determine the probability of the motifs occurring by chance in the sequences, the SMILE software was used [30]. This algorithm allows dealing with structured motifs eventually associated by some distance constraints.

RESULTS

Identification of IRP-like proteins in *Arabidopsis*

In order to determine whether the animal IRE/IRP regulatory system may have a counterpart in plants, we first tried to identify IRP1 and IRP2 homologues in the *Arabidopsis* genome. We identified three genes encoding aconitate hydratase, named *ACO1* (At4g35830), *ACO2* (At4g26970) and *ACO3* (At2g05710). *ACO1* corresponds to the gene previously identified by Peyret et al. [9]. The two others are identical with the genes recently identified by Moeder et al. [20]. The three proteins are closely related, share more than 90 % similarity and have approx. 80 % similarity with IRP1 and IRP2 (Figure 1). The three cysteine residues (indicated by squares on Figure 1) in the IRP1 sequence, involved in the Fe-S cluster formation, are completely conserved in the three plant ACO proteins, suggesting that they could associate a cluster, and could have an ACO activity. The crystal structure of the IRP1–ferritin H IRE complex allowed us to identify amino acids directly interacting with the RNA loop ([31]; indicated by stars on Figure 1). Interestingly, most of these residues are conserved in the three plant ACO proteins (Figure 1), raising the hypothesis that plant ACO could bind IRE sequences.

Isolation of *aco* loss-of-function mutants

To investigate the involvement of *Arabidopsis ACO* genes in ferritin regulation, we have isolated knockout mutants in the three corresponding genes from the Salk Institute [21] (for *ACO2*: line Salk054196, and for *ACO3*: line Salk013368) and the GABI-Kat [22] (for *ACO1*: line 138A08) collections. In the mutants, the two T-DNA flanking sequences were determined. The three mutants were named *aco1-1*, *aco2-1* and *aco3-1*. In the three mutant lines, the T-DNA were found to be inserted as an inverted tandem (Figure 2A). In *aco1-1*, the insertion is located in the 14th exon of the gene, and led to a small deletion of 5 bp, and to the insertion of 12 and 8 bp extra sequences at the 5′- and 3′-junctions respectively. In *aco2-1*, the insertion is located in the 6th exon, and led to a 413 bp deletion, and to the insertion of 12 bp extra sequence at the 3′-junction. In *aco3-1* mutant, the insertion was found to be located in the 5th exon, and led to a deletion of 8 bp, and to the addition of 5 bp extra sequence at the 3′-junction. The *aco3-1* line has been previously described by Moeder et al. [20] and was named KO-661 [20]. Lines homozygous for the disruption were isolated, and used for further studies. When the mutants were grown in a greenhouse, or in hydroponic cultures under controlled conditions, they displayed no macroscopic phenotype. Furthermore, changes in environmental parameters, such as light intensity or iron concentration in the culture solution, did not lead to any obvious phenotype (results not shown).

The expression of the three *ACO* genes was investigated in the *aco* mutant backgrounds by Northern blot with specific probes corresponding to the three genes (Figure 2B). In each mutant, the transcript corresponding to the mutated gene was undetectable, indicating that the mutants isolated are true knockout lines. The relative mRNA accumulation of the two remaining genes was not affected in any of the three mutants (Figure 2B). This result indicates that the disruption of an *ACO* gene does not alter the expression of the two other genes.

ACO genes encode aconitase, a key enzyme in the tricarboxylic acid cycle located in the mitochondria. To determine whether these genes could encode cytosolic ACO, both cytosolic and mitochondrial ACO activities were measured from 10-day-old plants grown in liquid medium. Mitochondrial matrix and cytosolic extracts were prepared, and the ACO activity was measured in each extract. The contamination of the cytosolic extract with mitochondrial proteins was determined by measuring the activity of the matrix-specific enzyme citrate synthase. In all experiments, the contamination of the cytosolic extracts by matrix mitochondria was estimated to be less than 5 % (results not shown). In the *aco1-1* mutant, the cytosolic and mitochondrial ACO activities were reduced by approx. 75 and 20 % respectively when compared with wild-type plants. In *aco3-1*, the reduction was approx. 25 % for the cytosolic and 55 % for the mitochondrial activities. The cytosolic ACO activity was not affected in the *aco2-1* background, whereas the mitochondrial activity was reduced by 20 % (Figure 2C). The mutations affected the ratio between mitochondrial and cytosolic activities. This indicates that, under our experimental conditions, ACO1 is mainly involved in the cytosolic activity, and ACO3 is responsible for the majority of the mitochondrial activity.

Expression of *ACO* genes in *Arabidopsis*

The expression pattern of the three *ACO* genes *in planta* was investigated. Total RNA extracted from seeds, roots, leaves, stems, caulinary leaves and flowers was analysed by Northern blot hybridization using the *ACO*-specific probes (Figure 3). The three genes present a very similar expression pattern, being expressed in all organs, except in the seeds, where *ACO1* mRNA accumulation was undetectable, and *ACO2* and *ACO3* genes were weakly expressed. *ACO1* mRNA was more abundant in roots, stems and caulinary leaves. The highest level of expression of *ACO2* was detected in roots, caulinary leaves and flowers.

To gain further insight regarding the potential IRP activity of the proteins encoded by the *ACO* genes, we first investigated the expression of the ACO genes under standard, iron-excess and iron-starved conditions (Figure 4). Under iron-excess conditions, the abundance of the *AtFer1* transcript increased rapidly. By contrast, the expression of the three ACO genes was not affected by this treatment (Figure 4A). Under iron-deficient condition, the mRNA corresponding to the iron-starvation-inducible gene *IRT1* [25,32] accumulated 2 days after application of the treatment. Under such conditions, the mRNA abundance of *ACO3* was not significantly affected compared with standard iron nutrition conditions, whereas those corresponding to *ACO1* and *ACO2* were slightly decreased after 3 days of starvation (Figure 4B).

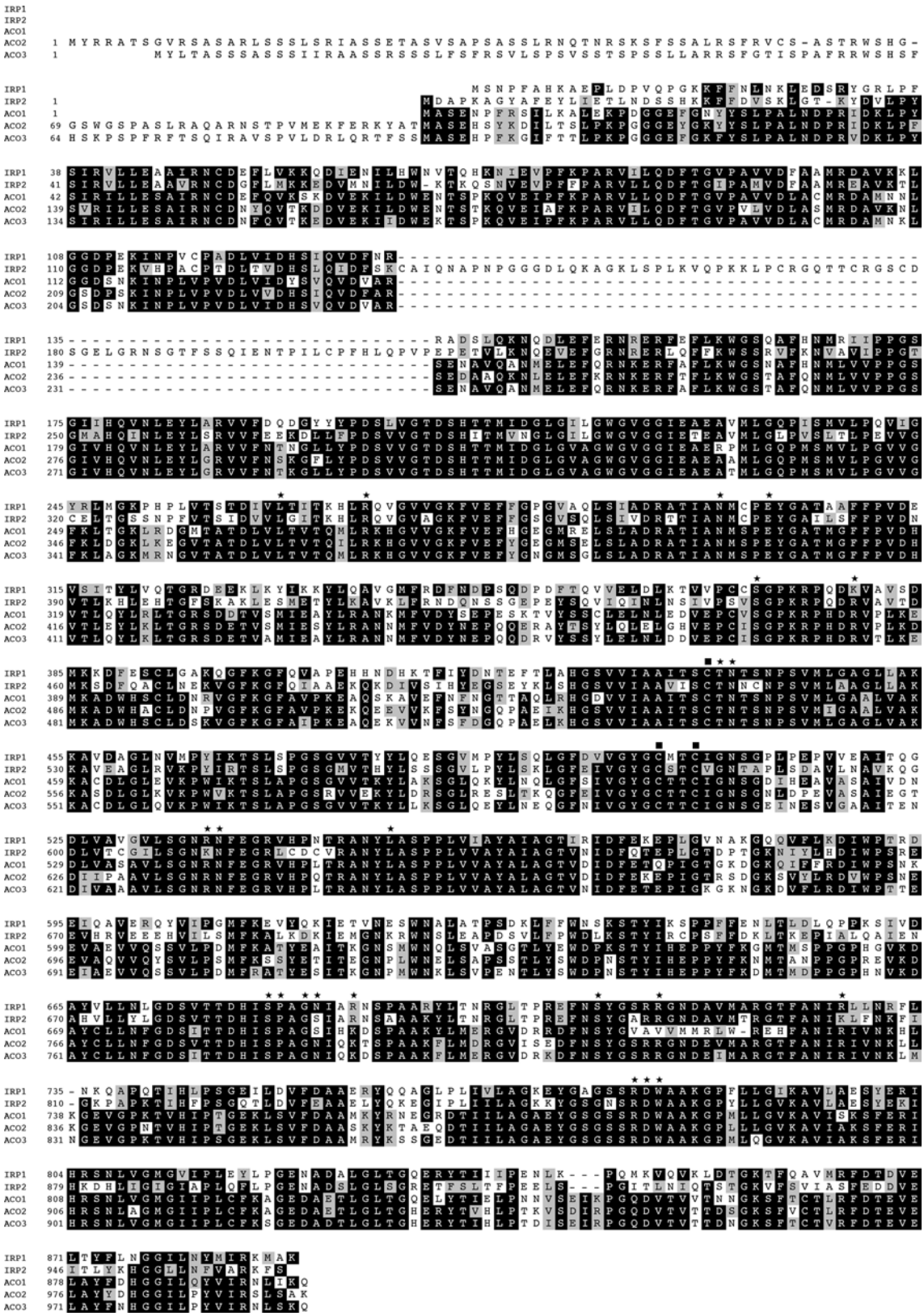

Figure 1 Sequence alignment of the deduced *Arabidopsis* ACOs with human IRP1 and IRP2

The human IRP1 (GenBank® accession number NP002188) and IRP2 (GenBank® accession number NP004127) were aligned with their *Arabidopsis* homologues At4g35830 (ACO1), At4g26970 (ACO2) and At2g05710 (ACO3). Identical and similar residues between at least three proteins are boxed in black and grey respectively. Gaps were introduced to maximize alignment. Amino acids are numbered from the translational start methionine. Star symbols indicate amino acids directly interacting with the RNA loop of the IRE [31]. The three cysteine residues involved in the 4Fe-4S cluster formation in IRP1 are indicated by closed squares.

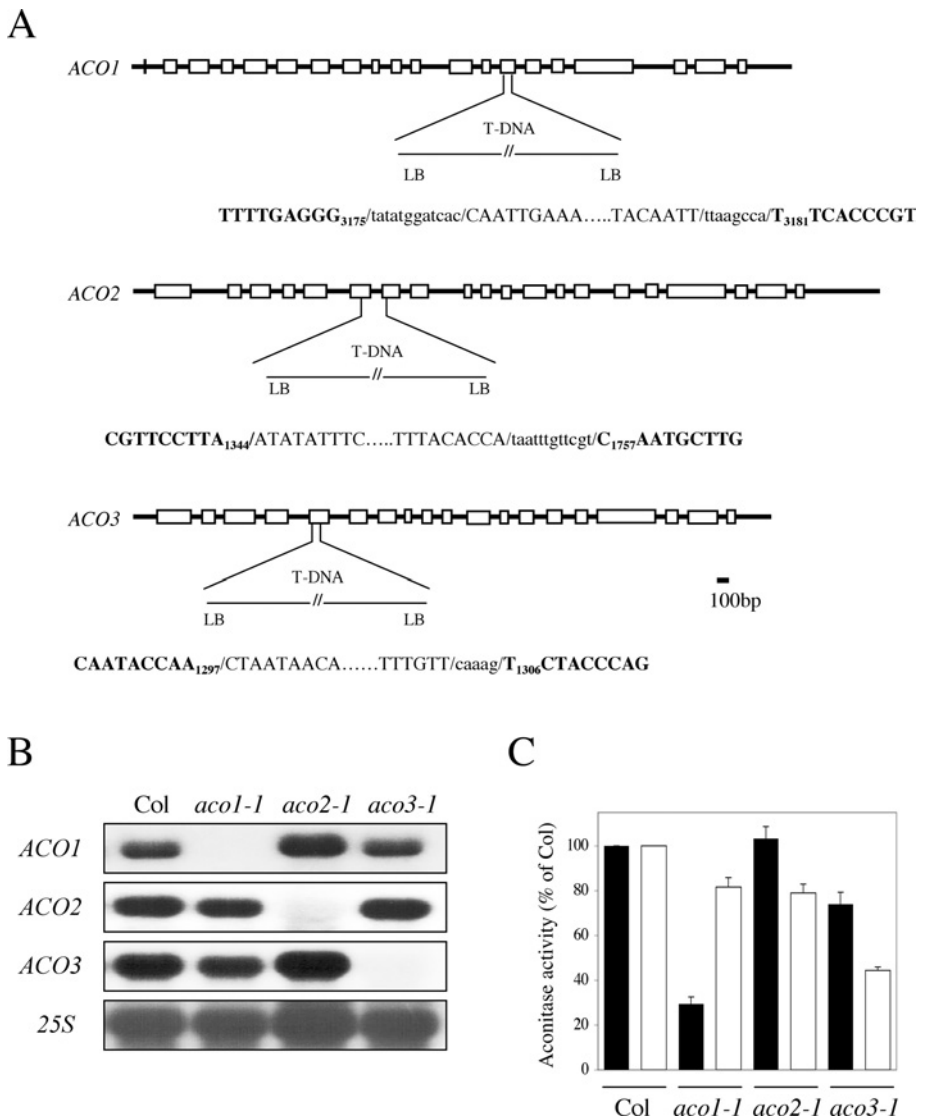

Figure 2 Isolation of *aco* knockout mutants

(**A**) Characterization of the *aco1-1*, *aco2-1* and *aco3-1* mutant lines. The diagram illustrates the site of insertion on the T-DNA in the different genes. Boxes and lines represent exons and introns respectively. The gene/T-DNA junction sequences are indicated. The gene sequences are indicated in boldface, the T-DNA sequences are in upper-case, and additional sequences found at the junctions are in lower-case. LB, left border of the T-DNA. Numbering is given relative to the first codon of the translation initiation site. (**B**) Expression of *ACO* genes in wild-type and *aco* mutants. Wild-type *Arabidopsis* (Col), *aco1-1*, *aco2-1* and *aco3-1* plantlets were grown for 10 days in liquid medium. RNA was analysed by Northern blotting and hybridized successively with the *ACO1*, *ACO2*, *ACO3* and *25S* probes. *25S* RNA abundance was shown as loading control. (**C**) Effect of the mutations on cytosolic and mitochondrial ACO activities. Plants were grown as described in (**B**). Cytosolic and matrix extracts were prepared, and the ACO activities were measured. Results are presented as the percentage of the cytosolic (black bars) and mitochondrial (white bars) ACO activities measured for Col plants. Bars correspond to the standard deviation from three independent experiments.

In animal cells, the switch between cytosolic ACO and IRP activity is associated with a decrease in the cytosolic ACO activity. To determine whether such a switch may occur in plants, we investigated whether iron addition or depletion may lead to a modulation of the cytosolic ACO activity. ACO activity was measured on 10-day-old plants grown in liquid medium, under control conditions (standard medium), 3 h after the addition of iron citrate (final concentration 300 μM), and after 1 day of growth in an iron-depleted medium. Cytosolic and mitochondrial ACO activities were measured in wild-type and in the three *aco* mutants (Figure 4C). In wild-type plants, the iron treatment led to a small increase in the cytosolic ACO activity of approx. 25 %. Iron starvation did not significantly modulate the activity. In the three *aco* mutants, the effects of iron addition and depletion on the cytosolic ACO activity were similar to those observed in wild-type

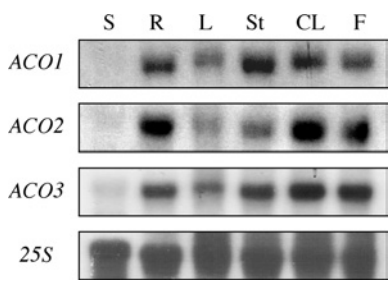

Figure 3 Expression of ACO genes in the different organs of *Arabidopsis*

Plants were grown under hydroponic conditions for 5 weeks. Total RNA was extracted from seeds (S), roots (R), rosette leaves (L), stems (St), caulinary leaves (CL) and flowers (F), and analysed by Northern blot as described in the legend to Figure 2.

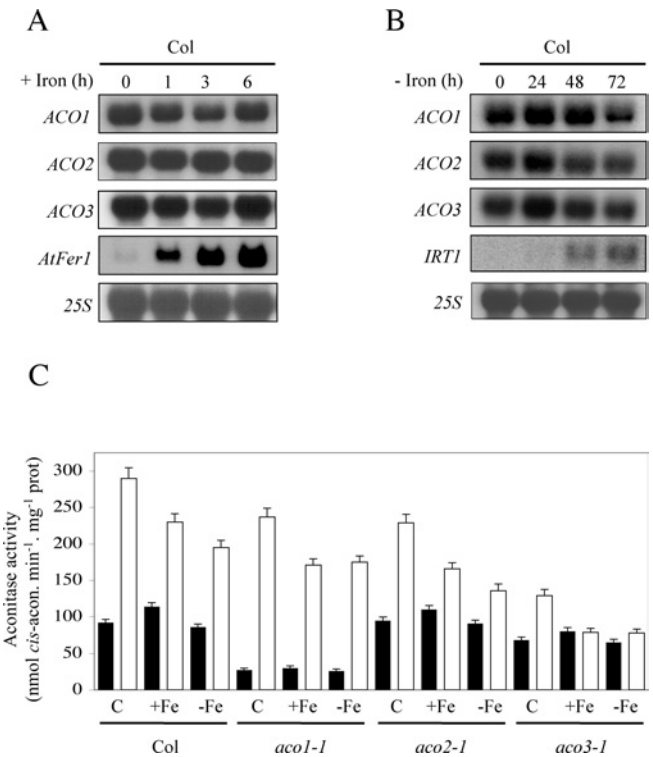

Figure 4 Effect of iron nutrition on ACO gene expression and ACO activities

(**A**) Effect of excess iron on *ACO* mRNA accumulation. Wild-type plantlets (Col) were grown as described in the legend to Figure 2. Iron citrate (final concentration 300 μM) was added, and plantlets were collected before (0) and 1, 3 and 6 h after iron addition. A Northern blot was performed as described in the legend to Figure 2. The mRNA abundance of *AtFer1* was used as a positive control of the iron treatment. (**B**) Effect of iron depletion on *ACO* mRNA accumulation. Col plantlets were grown for 7 days as described in the legend to Figure 2, and transferred to a medium without iron. Plantlets were collected before (0) and 24, 48 and 72 h after the transfer. A Northern blot was performed as described in the legend to Figure 2. The mRNA abundance of *IRT1* was used as a positive control of the treatment. (**C**) Effect of iron status on ACO activities. Col, *aco1-1*, *aco2-1* and *aco3-1* plantlets were grown for 10 days in liquid medium (C), 300 μM iron citrate was added for 3 h (+Fe), or plantlets were grown for an additional day in iron-free medium (–Fe). Cytosolic and matrix extracts were prepared, and the cytosolic (black bars) and mitochondrial (white bars) ACO activities were measured. Results are means±S.D. for three independent experiments.

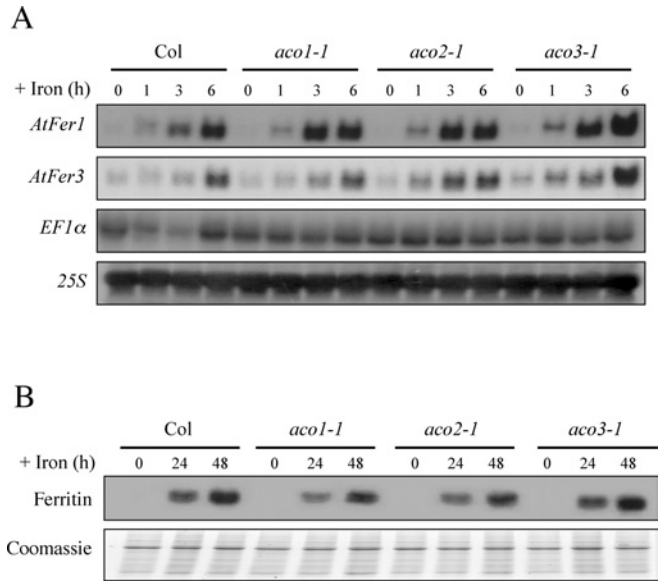

Figure 5 Effect of *aco* mutations on ferritin expression

(**A**) *AtFer1* and *AtFer3* mRNA abundance in *aco* mutants. Col, *aco1-1*, *aco2-1* and *aco3-1* plantlets were grown for 10 days in liquid medium. Iron citrate was added (300 μM final concentration), and plantlets were collected before (0) and 1, 3 and 6 h after the treatment. RNA was extracted, analysed by Northern blotting, and hybridized successively with the *AtFer1*, *AtFer3*, *EF1α* and *25S* probes. *EF1α* mRNA and *25S* RNA abundance were used as loading controls. (**B**) Effect of the mutation on ferritin protein accumulation in response to iron. Col, *aco1-1*, *aco2-1* and *aco3-1* plantlets were grown for 10 days in liquid medium. Iron citrate was added (300 μM final concentration), and plantlets were collected before (0), 24 h and 48 h after the treatment. Total protein was extracted. Protein extracts (10 μg) were loaded for each lane. A polyclonal serum (1:20000 dilution) raised against AtFer1 protein was used for immunodetection. A Coomassie Blue-stained gel is shown as the loading control.

plants. Both iron starvation and addition led to a slight decrease in mitochondrial ACO activity in all the genetic backgrounds.

Taken together, our results indicate that the modulation of the plant iron status did not strongly affect the expression of *ACO* genes in *Arabidopsis*. Moreover, cytosolic ACO activity was not greatly affected by iron addition or depletion. In the three loss-of-function mutants, the modulation of the cytosolic ACO activity in response to the iron status was the same as that in wild-type, suggesting that none among ACO1, ACO2 and ACO3 activities is strongly affected by iron.

Ferritin gene expression in *aco* mutants

The involvement of *Arabidopsis* ACO in the regulation of iron-responsive gene expression was finally investigated by analysing the expression of two ferritin genes in the different *aco* genetic backgrounds. The *AtFer1* and *AtFer3* genes were chosen since the corresponding mRNA and protein quickly accumulate in response to iron addition [12,13,33]. Moreover, in animal cells, ferritin genes are one of the primary targets of the IRE/IRP regulation. We first determined the kinetics of *AtFer1* and *AtFer3* mRNA accumulation in the wild-type and in the three *aco* mutants in response to excess iron (Figure 5A). In none of the mutants was the accumulation of the two ferritin mRNA affected. The ferritin protein accumulation was also investigated in the three genetic backgrounds (Figure 5B). Total protein extracts were prepared before, 24 h and 48 h after iron addition. The same level of ferritin accumulated in the three mutants compared with the wild-type. These results show that ACO1, ACO2 and ACO3 are not involved in the regulation of plant ferritin expression in response to iron, either at the transcriptional or at the post-transcriptional level.

Functional redundancy between the cytosolic ACO proteins

Our results indicated that ACO2 protein does not have cytosolic ACO activity, at least under our experimental conditions (Figure 4C). On the other hand, in *aco1-1* and *aco3-1* mutants, the cytosolic ACO activity is reduced by approx. 75 and 25 % respectively in comparison with the wild-type (Figures 2 and 4C), indicating that the corresponding proteins represent the two major sources of plant cytosolic ACO activity. The expression pattern of *ACO1* and *ACO3* genes are very similar (Figure 3), suggesting that the two proteins may, at least partially, be redundant. Thus it cannot be excluded that the absence of modulation of ferritin gene expression in the single *aco1-1* and *aco3-1* mutants (Figure 5) was due to a compensation mechanism between ACO1 and ACO3. In order to isolate and characterize a double *aco1-aco3* mutant, the progenies of plants homozygous for one mutation and heterozygous for the other (namely *aco1aco1-ACO3aco3* and *ACO1aco1-aco3aco3*) were sown, and the genotype of the progeny was analysed by PCR to detect the wild-type and mutant alleles. More than 100 plants from the two progenies were

A

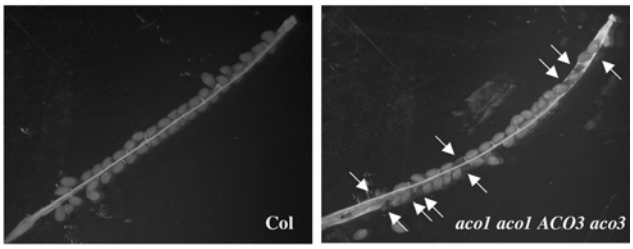

B

Genotype	Total seeds	Aborted seeds	Proportion aborted (%)
Col	136	1	0.73
ACO1 aco1-1 aco3-1 aco3-1	171	41	23.97
aco1-1 aco1-1 ACO3 aco3-1	328	85	25.91

Figure 6 The double mutant *aco1-1 aco3-1* is lethal

(**A**) Aborted seeds present in siliquae of a plant mutant in *ACO1* gene and heterozygous at the *ACO3* locus. Wild-type (Col) and mutant (genotype *aco1-1 aco1-1 ACO3 aco3-1*) plants were grown in a greenhouse and siliquae were collected just before dehiscence. Siliquae were opened and seeds were examined using a binocular microscope. All the seeds were normal in Col plants (left), whereas some were aborted in the mutant (right; aborted seeds are indicated by arrows). (**B**) Proportion of aborted seeds in the progeny of plants mutant at one locus, and heterozygous at the second. Wild-type (Col) and mutant plants (genotype *aco1-1 aco1-1 ACO3 aco3-1* and *ACO1 aco1-1 aco3-1 aco3-1*) were grown in a greenhouse, and seeds were collected. The proportion of aborted seeds was estimated visually using a binocular microscope.

analysed, but we failed to identify a double *aco1aco1-aco3aco3* mutant, suggesting that a mutation in both *ACO1* and *ACO3* genes is lethal. Moreover, when examining the seeds in the siliquae of *aco1aco1*-ACO3*aco3* and ACO1*aco1-aco3aco3* plants, some aborted seeds were systematically observed (Figure 6A). The proportion of aborted seeds in the progeny of the two parental lines was close to 25 %, a value expected for a lethal double mutation (Figure 6B). Our results indicate that ACO1 and ACO3 protein activities are required for the development of the embryo, or for the proper development of the seed and, as a consequence, we are unable to study ferritin expression in the double *aco1-aco3* mutant.

Identification of IRE and potential bacterial ACO-binding sites in the *Arabidopsis* genome

Our results (Figure 5) show clearly that *Arabidopsis* ACOs are not involved in the transcriptional activation of *AtFer1* and *AtFer3* ferritin genes. However, it must be pointed out that most of the residues known to be essential for the RNA-binding activity of rabbit IRP1 are conserved in *Arabidopsis* ACO proteins (Figure 1). Such an important amino acid conservation is intriguing, and it indicates that a nucleotide-binding activity of these proteins has to be considered. These essential residues for the IRP activity are also conserved in the bacterial ACO protein that has been shown to bind to motifs unrelated to IRE [18]. The exact recognized motif (or sequence) by bacterial ACO is still unknown, but some conserved elements have been identified in the 3′-UTR of *acnA* and *acnB* genes [18]. The high conservation of residues among animal, plant and bacterial proteins suggests that plant ACO may also have an RNA binding activity. This hypothesis is supported by the recent work of Moeder et al. [20], which shows that *Arabidopsis* ACO1 protein is able to bind to the 5′-UTR of *CSD2* superoxide dismutase transcript.

To further study the potential involvement of plant ACO as a nucleotide-binding protein, we took advantage of the availability of the whole *Arabidopsis* genome sequence to look for potential binding sites in the 5′- and 3′-UTR of all the transcripts. For this bioinformatic search, we used the animal IRE, and the sequences identified in *Escherichia coli acnA* and *acnB* genes [18]. In animals, IREs are stem-loops made of 30 nt with a bulge. The loop has a conserved sequence, 5′-CAGUGN-3′, N usually being a pyrimidine [34]. We performed a search with the loop consensus sequence surrounded by a stem consisting of at least five bases in 5′ complementary to the five bases located in 3′. Using this rule, we found only four genes containing a putative IRE, one gene with the sequence in the 5′-UTR, and the three others in the 3′-UTR (Table 1). The binding site of the bacterial ACO is still unknown, but from the sequence homologies between the 3′-UTRs of the two target genes *acnA* and *acnB*, Tang and Guest [18] have suggested that two paired motifs, namely ACACAAUGC and CAUUUU, may, at least partly, be involved in the formation of ACO-binding sites. We searched for these two paired motifs in the *Arabidopsis* genome and found them in the 5′-UTR of two genes and in the 3′-UTR of four others (Table 1). Because the probability of finding them in UTR sequence is likely more than 99 % due to chance, as indicated by the SMILE software [30], such sequences are unlikely to be functional.

DISCUSSION

To directly address the question of a potential link between plant cytosolic ACO and the regulation of ferritin expression, we took advantage of the availability of the *A. thaliana* genome sequence. We searched for IRP1 and IRP2 homologues, and three proteins

Table 1 Putative IRE and bacterial ACO-binding sites in the UTRs of *A. thaliana* genes

For each accession number, the location (in the 5′- or 3′-UTR) of the putative element in the transcript is indicated. For IRE sequence, the corresponding sequence found in the database is given. The bases of the IRE consensus are indicated in boldface. The AGI (*Arabidopsis* Genome Initiative) number, and function of the corresponding genes are indicated.

cis-Element	Location	Sequence	AGI	Function
IRE	3′-UTR	**C**UGGAU**CAGUGG**AUCUA	At1g63490	Jumonji domain-containing protein
	3′-UTR	**C**AUAAU**CAGUGU**AUUAU	At3g02520	14-3-3 protein
	5′-UTR	**C**AAAAU**CAGUGA**AUUUU	At3g54130	Josephin protein family
	3′-UTR	**C**UUGUG**CAGUGG**CACAA	At3g61380	Unknown
acn-Binding domain	5′-UTR	ACACAAUGC and CAUUUU	At1g35510	Unknown
	5′-UTR	ACACAAUGC and CAUUUU	At2g40460	Proton-dependent oligopeptide transporter
	3′-UTR	ACACAAUGC and CAUUUU	At3g10220	Tubulin folding cofactor B
	3′-UTR	ACACAAUGC and CAUUUU	At5g01450	Unknown
	3′-UTR	ACACAAUGC and CAUUUU	At5g28150	Unknown
	3′-UTR	ACACAAUGC and CAUUUU	At5g63780	Zinc finger

(ACO1–3) were identified. These IRP-like proteins were found to encode mitochondrial ACO (Figures 2 and 4), a result consistent with studies that found the three ACO proteins in the mitochondrial proteome [35]. In animals, mitochondrial and cytosolic ACOs are encoded by distinct genes [36,37]. It is not the case in *Saccharomyces cerevisiae*, in which a unique gene encodes both mitochondrial and cytosolic ACOs [38,39]. In plants, several reports indicate that, as in yeast, both mitochondrial and cytosolic ACOs are encoded by the same genes, suggesting a dual targeting of the proteins [40–42]. Therefore the question we had to address was whether or not the three identified ACOs were targeted to the cytosol. The contribution of each ACO protein to the cytosolic ACO activity was estimated from the analysis of the *aco* knockout mutants (Figure 2), and suggests that ACO1 and ACO3 are the two major proteins displaying a cytosolic ACO activity. ACO2, which is present in the mitochondria [35,43,44], may not be targeted to the cytosol. Alternatively, our experimental conditions may not reveal the cytosolic ACO activity of this protein. Our results bring additional information to the work of Moeder et al. [20], who determined the total (cytosolic + mitochondria matrix) ACO activity in various *aco* mutant genetic backgrounds. It has also to be mentioned that the *aco1-1* and *aco2-1* mutants we have characterized in the present study are alleles different from those used by Moeder et al. [20].

Our major goal was to determine whether or not cytosolic ACO is involved in the regulation of ferritin expression in plants. To address this question, we first studied the effect of the plant iron status on *ACO* gene expression (Figure 4). At the mRNA level, neither iron excess nor iron depletion modulated the expression of ACO genes. Moreover, when measuring the effect of iron treatments on the cytosolic ACO activity, no strong variations were observed in wild-type, or in the mutants (Figure 4). Consistent with an IRP1–cytosolic ACO switch, a variation of the plant iron status should have led to a modulation of the cytosolic ACO activity by affecting the Fe-S assembly of the protein. Finally, the direct evidence that *Arabidopsis* ACOs are not involved in the regulation of ferritin expression was provided by studying the expression of two ferritin genes at the mRNA and protein levels in the *aco* mutant genetic backgrounds. In the three *aco* mutants, both the level of *AtFer1* and *AtFer3* transcript accumulated, and the amounts of ferritin subunit were identical with those detected in the wild-type. A potential functional redundancy between ACO1 and ACO3 could explain the lack of effect of the mutations on ferritin expression. However, we did not observe any compensation between the three ACO genes (Figure 2A), since the mutation in one gene did not affect the expression of the two others. The remaining activity in the *aco1-1* mutant (probably due to ACO3 activity) could be sufficient to explain the absence of modulation of ferritin expression. We therefore intended to isolate a double *aco1-1 aco3-1* mutant, but failed to do so, as the presence of the two mutations leads to the abortion of seeds. This result indicates that the cytosolic ACO activity is essential for the proper formation of the embryo or for the development of the seed.

Besides the question of the involvement of cytosolic ACO in the regulation of iron metabolism in plants, our work provides tools to study the impact of disturbing the glyoxylate and/or tricarboxylic acid cycles on plant growth and metabolism. The relative contribution of each ACO isoform to the mitochondrial and cytosolic ACO activities, to the metabolism [42], to the regulation of oxidative stress and to the establishment of defence against pathogens [20,45] could be studied with the loss-of-function mutants.

As a complementary approach to determine whether the IRE/IRP1–cytosolic ACO switch may occur or not in plants, we performed a bioinformatic search for putative ACO RNA-binding sites in the 5′- and 3′-UTR of *Arabidopsis* transcripts. Only ten genes contain one of these sequences (Table 1). Among them, four genes contained a putative IRE sequence, and six genes contained the two consensus sequences [18] found in the bacterial ACO-regulated genes. The low number of genes containing these elements raises therefore the question of their significance. Four genes encode unknown proteins, and among the others, none of them is obviously related to iron metabolism.

Recent results show that plant cytosolic ACO proteins may have an RNA binding activity. Indeed, *Arabidopsis* ACO1 is able to bind to the 5′-UTR of the *CSD2* superoxide dismutase transcript [20]. This result raises the interesting point that, as in animals, plant cytosolic ACO may have an RNA binding activity. However, the *CSD2* ACO-binding site is neither an IRE nor a bacterial ACO-binding site [20]. Our bioinformatic analysis, which indicates that animal and bacterial *cis*-acting sequences are probably not functional in plants, is consistent with this result, since the *CSD2* gene was not detected by our analysis. These results suggest that the potential RNA binding activity of plant ACO proteins does not involve a canonical *cis*-acting sequence, but would be more likely related to the secondary structure of the RNA region. The identification of the nucleotides involved in the *CSD2* ACO1-binding site, and the search for other transcripts able to bind ACO1 will be of primary importance in the future. Even more important will be the demonstration that this *in vitro* binding activity does exist *in vivo* and participates in the regulation of so far unknown biological functions.

This work was funded by Institut National de la Recherche Agronomique and Centre National de la Recherche Scientifique, and by the Action Concertée Incitative 'Biologie Cellulaire Moléculaire et Structurale' number BCMS166 from the Ministère de l'Education Nationale, de l'Enseignement Supérieur et de la Recherche. N. A. and K. R. were supported by a thesis fellowship from the Ministère de l'Education Nationale, de l'Enseignement Supérieur et de la Recherche.

REFERENCES

1 Guerinot, M. L. and Yi, Y. (1994) Iron: nutritious, noxious, and not readily available. Plant Physiol. **104**, 815–820
2 Noctor, G. and Foyer, C. H. (1998) Ascorbate and glutathione: keeping active oxygen under control. Annu. Rev. Plant Physiol. Plant Mol. Biol. **49**, 249–279
3 Harrison, P. M. and Arosio, P. (1996) The ferritins: molecular properties, iron storage function and cellular regulation. Biochim. Biophys. Acta **1275**, 161–203
4 Hentze, M. W. and Kuhn, L. C. (1996) Molecular control of vertebrate iron metabolism: mRNA-based regulatory circuits operated by iron, nitric oxide, and oxidative stress. Proc. Natl. Acad. Sci. U.S.A. **93**, 8175–8182
5 Klausner, R. D., Rouault, T. A. and Harford, J. B. (1993) Regulating the fate of mRNA: the control of cellular iron metabolism. Cell **72**, 19–28
6 Hirling, H., Henderson, B. R. and Kuhn, L. C. (1994) Mutational analysis of the [4Fe-4S]-cluster converting iron regulatory factor from its RNA-binding form to cytoplasmic aconitase. EMBO J. **13**, 453–461
7 Gardner, P. R., Raineri, I., Epstein, L. B. and White, C. W. (1995) Superoxide radical and iron modulate aconitase activity in mammalian cells. J. Biol. Chem. **270**, 13399–13405
8 Rouault, T. A. (2006) The role of iron regulatory proteins in mammalian iron homeostasis and disease. Nat. Chem. Biol. **2**, 406–414
9 Peyret, P., Perez, P. and Alric, M. (1995) Structure, genomic organization, and expression of the *Arabidopsis thaliana* aconitase gene. Plant aconitase show significant homology with mammalian iron-responsive element-binding protein. J. Biol. Chem. **270**, 8131–8137
10 Navarre, D. A., Wendehenne, D., Durner, J., Noad, R. and Klessig, D. F. (2000) Nitric oxide modulates the activity of tobacco aconitase. Plant Physiol. **122**, 573–582
11 Murgia, I., Delledonne, M. and Soave, C. (2002) Nitric oxide mediates iron-induced ferritin accumulation in *Arabidopsis*. Plant J. **30**, 521–528
12 Petit, J. M., Briat, J. F. and Lobréaux, S. (2001) Structure and differential expression of the four members of the *Arabidopsis thaliana* ferritin gene family. Biochem. J. **359**, 575–582
13 Arnaud, N., Murgia, I., Boucherez, J., Briat, J. F., Cellier, F. and Gaymard, F. (2006) An iron-induced nitric oxide burst precedes ubiquitin-dependent protein degradation for *Arabidopsis AtFer1* ferritin gene expression. J. Biol. Chem. **281**, 23579–23588

14 Verniquet, F., Gaillard, J., Neuburger, M. and Douce, R. (1991) Rapid inactivation of plant aconitase by hydrogen peroxide. Biochem. J. **276**, 643–648
15 Lescure, A. M., Proudhon, D., Pesey, H., Ragland, M., Theil, E. C. and Briat, J. F. (1991) Ferritin gene transcription is regulated by iron in soybean cell cultures. Proc. Natl. Acad. Sci. U.S.A. **88**, 8222–82226
16 Rothenberger, S., Mullner, E. W. and Kuhn, L. C. (1990) The mRNA-binding protein which controls ferritin and transferrin receptor expression is conserved during evolution. Nucleic Acids Res. **18**, 1175–1179
17 Brown, P. H., Daniels-McQueen, S., Walden, W. E., Patino, M. M., Gaffield, L., Bielser, D. and Thach, R. E. (1989) Requirements for the translational repression of ferritin transcripts in wheat germ extracts by a 90-kDa protein from rabbit liver. J. Biol. Chem. **264**, 13383–13386
18 Tang, Y. and Guest, J. R. (1999) Direct evidence for mRNA binding and post-transcriptional regulation by *Escherichia coli* aconitases. Microbiology **145**, 3069-3079
19 Tang, Y., Quail, M. A., Artymiuk, P. J., Guest, J. R. and Green, J. (2002) *Escherichia coli* aconitases and oxidative stress: post-transcriptional regulation of sodA expression. Microbiology **148**, 1027–1037
20 Moeder, W., Del Pozo, O., Navarre, D. A., Martin, G. B. and Klessig, D. F. (2006) Aconitase plays a role in regulating resistance to oxidative stress and cell death in *Arabidopsis* and *Nicotiana benthamiana*. Plant Mol. Biol. **63**, 273–287
21 Alonso, J. M., Stepanova, A. N., Leisse, T. J., Kim, C. J., Chen, H., Shinn, P., Stevenson, D. K., Zimmerman, J., Barajas, P., Cheuk, R., et al. (2003) Genome-wide insertional mutagenesis of *Arabidopsis thaliana*. Science **301**, 653–657
22 Rosso, M. G., Li, Y., Strizhov, N., Reiss, B., Dekker, K. and Weisshaar, B. (2003) An *Arabidopsis thaliana* T-DNA mutagenized population (gabi-kat) for flanking sequence tag-based reverse genetics. Plant Mol. Biol. **53**, 247–259
23 Cellier, F., Conejero, G., Ricaud, L., Luu, D. T., Lepetit, M., Gosti, F. and Casse, F. (2004) Characterization of AtCHX17, a member of the cation/H^+ exchangers, CHX family, from *Arabidopsis thaliana* suggests a role in K^+ homeostasis. Plant J. **39**, 834–846
24 Lobréaux, S., Hardy, T. and Briat, J. F. (1993) Abscisic acid is involved in the iron-induced synthesis of maize ferritin. EMBO J. **12**, 651–657
25 Vert, G., Grotz, N., Dedaldechamp, F., Gaymard, F., Guerinot, M. L., Briat, J. F. and Curie, C. (2002) IRT1, an *Arabidopsis* transporter essential for iron uptake from the soil and for plant growth. Plant Cell **14**, 1223–1233
26 Schaffner, W. and Weissmann, C. (1973) A rapid, sensitive, and specific method for the determination of protein in dilute solution. Anal. Biochem. **56**, 502–514
27 Lobréaux, S., Massenet, O. and Briat, J. F. (1992) Iron induces ferritin synthesis in maize plantlets. Plant Mol. Biol. **19**, 563–575
28 Laemmli, U. K. (1970) Cleavage of structural proteins during the assembly of the head of bacteriophage T4. Nature **227**, 680–685
29 Dellagi, A., Rigault, M., Segond, D., Roux, C., Kraepiel, Y., Cellier, F., Briat, J. F., Gaymard, F. and Expert, D. (2005) Siderophore-mediated upregulation of *Arabidopsis* ferritin expression in response to *Erwinia chrysanthemi* infection. Plant J. **43**, 262–272
30 Marsan, L. and Sagot, M. F. (2000) Algorithms for extracting structured motifs using a suffix tree with an application to promoter and regulatory site consensus identification. J. Comput. Biol. **7**, 345–362
31 Walden, W. E., Selezneva, A. I., Dupuy, J., Volbeda, A., Fontecilla-Camps, J. C., Theil, E. C. and Volz, K. (2006) Structure of dual function iron regulatory protein 1 complexed with ferritin IRE-RNA. Science **314**, 1903–1908
32 Eide, D., Broderius, M., Fett, J. and Guerinot, M. L. (1996) A novel iron-regulated metal transporter from plants identified by functional expression in yeast. Proc. Natl. Acad. Sci. U.S.A. **93**, 5624–5628
33 Gaymard, F., Boucherez, J. and Briat, J. F. (1996) Characterization of a ferritin mRNA from *Arabidopsis thaliana* accumulated in response to iron through an oxidative pathway independent of abscisic acid. Biochem. J. **318**, 67–73
34 Theil, E. C. (1994) Iron regulatory elements (IREs): a family of mRNA non-coding sequences. Biochem. J. **304**, 1–11
35 Heazlewood, J. L., Tonti-Filippini, J. S., Gout, A. M., Day, D. A., Whelan, J. and Millar, A. H. (2004) Experimental analysis of the *Arabidopsis* mitochondrial proteome highlights signaling and regulatory components, provides assessment of targeting prediction programs, and indicates plant-specific mitochondrial proteins. Plant Cell **16**, 241–256
36 Eanes, R. Z. and Kun, E. (1971) Separation and characterization of aconitate hydratase isoenzymes from pig tissues. Biochim. Biophys. Acta **227**, 204–210
37 Kennedy, M. C., Mende-Mueller, L., Blondin, G. A. and Beinert, H. (1992) Purification and characterization of cytosolic aconitase from beef liver and its relationship to the iron-responsive element binding protein. Proc. Natl. Acad. Sci. U.S.A. **89**, 11730–11734
38 Gangloff, S. P., Marguet, D. and Lauquin, G. J. (1990) Molecular cloning of the yeast mitochondrial aconitase gene (*aco1*) and evidence of a synergistic regulation of expression by glucose plus glutamate. Mol. Cell. Biol. **10**, 3551–3561
39 Regev-Rudzki, N., Karniely, S., Ben-Haim, N. N. and Pines, O. (2005) Yeast aconitase in two locations and two metabolic pathways: seeing small amounts is believing. Mol. Biol. Cell **16**, 4163–4171
40 Brouquisse, R., Nishimura, M., Gaillard, J. and Douce, R. (1987) Characterization of a cytosolic aconitase in higher plant cells. Plant Physiol. **84**, 1402–1407
41 De Bellis, L., Tsugeki, R., Alpi, A. and Nishimura, M. (1993) Purification and characterization of aconitase isoforms from etiolated pumpkin cotyledons. Physiol. Plant. **88**, 485–492
42 Carrari, F., Nunes-Nesi, A., Gibon, Y., Lytovchenko, A., Loureiro, M. E. and Fernie, A. R. (2003) Reduced expression of aconitase results in an enhanced rate of photosynthesis and marked shifts in carbon partitioning in illuminated leaves of wild species tomato. Plant Physiol. **133**, 1322–1335
43 Kruft, V., Eubel, H., Jansch, L., Werhahn, W. and Braun, H. P. (2001) Proteomic approach to identify novel mitochondrial proteins in *Arabidopsis*. Plant Physiol. **127**, 1694–1710
44 Millar, A. H., Sweetlove, L. J., Giege, P. and Leaver, C. J. (2001) Analysis of the *Arabidopsis* mitochondrial proteome. Plant Physiol. **127**, 1711–1727
45 Cots, J. and Widmer, F. (1999) Germination, senescence and pathogenic attack in soybean (*Glycine max* L.): identification of the cytosolic aconitase participating in the glyoxylate cycle. Plant Sci. **149**, 95–104

Received 15 December 2006/28 March 2007; accepted 16 April 2007
Published as Immediate Publication 16 April 2007, doi:10.1042/BJ20061874